

Article

Stochastic Levenberg–Marquardt Neural Network Implementation for Analyzing the Convective Heat Transfer in a Wavy Fin

R. S. Varun Kumar ¹, M. D. Alsulami ², I. E. Sarris ^{3,*}, G. Sowmya ⁴ and Fehmi Gamaoun ⁵

¹ Department of Mathematics, Amrita School of Engineering, Amrita Vishwa Vidyapeetham, Bengaluru 560035, India; rs_varun@blr.amrita.edu

² Department of Mathematics, College of Sciences and Arts at Alkamil, University of Jeddah, Jeddah 23218, Saudi Arabia; mdalsolami@uj.edu.sa

³ Department of Mechanical Engineering, University of West Attica, 12244 Athens, Greece

⁴ Department of Mathematics, M S Ramaiah Institute of Technology, Bangalore 560054, India

⁵ Department of Mechanical Engineering, College of Engineering, King Khalid University, Abha 61421, Saudi Arabia; fgamaoun@kku.edu.sa

* Correspondence: sarris@uniwa.gr

Abstract: The present research examines the steady, one-dimensional thermal distribution and heat transfer of a wavy fin. This heat transfer analysis considers convective effects as well as temperature-dependent thermal conductivity. Furthermore, a novel implementation of a neural network with backpropagated Levenberg–Marquardt algorithm (NN-BLMA)-based machine learning intelligent strategies is provided to interpret the heat transfer analysis of a convective wavy fin. The non-linear ordinary differential equation (ODE) of the study problem is converted into its non-dimensional form using the similarity transformation technique. The dimensionless equation obtained is then numerically explored via the Runge–Kutta–Fehlberg scheme. A data set for varying the pertinent parameters is generated, and an artificial neural network model is designed to estimate the heat transfer behavior of the wavy fin. The effectiveness of the proposed NN-BLMA is subsequently endorsed by analyses using a regression model, mean square error, and histograms. The findings of comprehensive computational parametric studies illustrate that the presented technique, NN-BLMA is an effective convergent stochastic numerical solver employed for the heat transfer model of the convective wavy fin. The wavy fin's temperature dispersion optimizes as the thermal conductivity parameter rises. Heat transfer rate is higher in wavy fin compared to rectangular fin.

Keywords: fin; temperature distribution; thermal conductivity; wavy fin; artificial neural network

MSC: 74A15; 68T01



Citation: Kumar, R.S.V.; Alsulami, M.D.; Sarris, I.E.; Sowmya, G.; Gamaoun, F. Stochastic Levenberg–Marquardt Neural Network Implementation for Analyzing the Convective Heat Transfer in a Wavy Fin. *Mathematics* **2023**, *11*, 2401. <https://doi.org/10.3390/math11102401>

Academic Editors: Elena Niculina Dragoi, Mircea Teodor Nechita and Yang Liu

Received: 9 March 2023

Revised: 12 May 2023

Accepted: 18 May 2023

Published: 22 May 2023



Copyright: © 2023 by the authors. Licensee MDPI, Basel, Switzerland. This article is an open access article distributed under the terms and conditions of the Creative Commons Attribution (CC BY) license (<https://creativecommons.org/licenses/by/4.0/>).

1. Introduction

The rapid progression of heat exchange associated with heat transfer mechanisms is required for many engineering applications. Fin arrangements are often utilized to expedite heat exchange on a surface. Fins are most frequently utilized in microelectronic equipment, including CPU heat sinks and optoelectronics, such as lasers. Fins are also used in thermal and electrical components to speed up heat transfer within them. Furthermore, they have been employed in a variety of advanced manufacturing operations such as computer processor cooling, air conditioning, oil transport pipelines, and so on. Gorla and Bakier [1] elucidated the heat transfer in a porous extended surface with the influence of radiation and convection. They concluded that the combined influence of these effects helps efficiently transfer excess heat from the fin's surface. Hoseinzadeh et al. [2] studied heat exchange in a rectangular cross-section porous fin under laminar flow conditions in a homogeneous medium. In their work, it is revealed that the convective mechanism influences the heat exchange in the fin. Venkitesh and Mallick [3] explained heat transport in

an annular-shaped porous fin with radiative impact. They determined that the fin material's thermal conductivity coefficient significantly impacted fin performance. The material noticeably increased the fin efficiency with a positive thermal conductivity coefficient over the material with a negative thermal conductivity coefficient. Madhura et al. [4] analyzed the change in temperature through a straight permeable fin under the effects of radiation and magnetic field. According to the findings of their investigation, the non-linear thermal conductivity variable improves the thermal performance and efficacy of the fin. Moreover, the fin's heat exchange rate optimizes as the magnetic and radiation parameters are boosted. Ndlovu and Moitsheki [5] examined the temperature distribution on a moving, straight, permeable extended surface. Their investigation findings show that as the convection-radiation parameter is increased, the fin rapidly releases heat to the surrounding air temperature. Wang et al. [6] studied heat transfer analysis in an inclined straight fin under convective and radiative effects conditions. They also discussed the heat transfer aspects in the influence of internal heat generation and the porous effect. Over the last several decades, research on fins has been executed with various temperature-dependent phenomena. In most studies, the heat transfer coefficient was often taken as a power function, and the thermal conductivity was considered constant or thermal dependent. Thermal distribution in a moving permeable extended surface was studied by Aziz and Khani [7] by using the homotopy analysis method. They considered the temperature-dependent thermal conductivity and discussed its impact on the fin's thermal variation. Sun and Ma [8] investigated the temperature distribution in a rectangular fin by taking the variable temperature-dependent thermal conductivity, convection, and internal heat generation effects. In their work, they discussed the consequence of the variable heat transfer coefficient on the fin performance. Dogonchi and Ganji [9] examined the heat generation impact in a moving extended surface with thermal conductivity and heat transfer coefficient dependent on temperature. Their work includes the assessment of various mechanisms of heat transfer and shows that increasing thermal conductivity variable levels result in a rise in the thermal distribution in the fin. Khan et al. [10] studied the convective-conductive-radiative heat transfer in a fin with temperature-dependent thermal conductivity. Their analysis shows that the estimated temperature's reliability rises with decreasing convective parameter values. Sarwe and Kulakarni [11] analyzed the heat transfer in a circular hyperbolic fin with thermal conductivity dependent on temperature. The findings of their investigation signify that increasing the value of the thermal conductivity parameter increases the thermal distribution.

A solid that undergoes heat exchange by conduction both within and between its boundaries and transferring energy by convection between its boundaries and surroundings is commonly referred to as an extended surface. They are frequently used in various applications, including refrigeration and numerous cooling systems in industries for air cooling and dehumidification. As the fins extend from the primary heat exchange surface, the difference in temperature between the fluid in the surrounding area and the fins significantly reduces. Roy and Mallick [12] analyzed the heat transmission in a longitudinal rectangular fin. They also considered the thermal variant surface emissivity and thermal conductivity. Ndlovu [13] studied the heat transfer process in a rectangular fin with convective and radiative heat exchange. He observed that a fin with a convective tip transmits heat to the surrounding fluid more rapidly than a fin with an insulated tip. Gouran et al. [14] explained the convection heat transmission through a moveable rectangular fin. According to their findings, higher cooling performance with straight fins occurs at high convective parameter values. Khan et al. [15] investigated the heat transfer analysis within a fin having a rectangular profile in the existence of convective and radiative environments. In their work, the thermal-dependent heat transfer coefficient and emissivity are taken into account. They concluded that the cooling process of the fin is aided by the constant discharge of heat from the fin surface via convection. Din et al. [16] examined the heat exchange in a rectangular fin with a stretching/shrinking property. They observed that the performance of the fin establishes an upsurge for shrinking and a diminution for expanding the fin

when convection occurs. There are many different sizes and types of fins. Researchers have examined and offered insights into fin parameters for a variety of fin configurations, including pin fins, circular, rectangular, triangular, trapezoidal, and concave parabolic fins. For instance, Sarwe and Kulkarni [17] probed the transfer of heat in an annular fin and presented the semi-analytical solution for the developed equation. They determined that larger levels of the thermal conductivity parameter result in greater fin efficiency. With the surface wet condition impact, Kumar and Sowmya [18] debriefed the thermal variation in the trapezoidal structured longitudinal fin. Their study investigates how thermal and heat energy changes vary in both dry and wet situations. The explanation for the thermal variation in the permeable exponential-shaped fin wetted with hybrid nanoliquid was presented by Abdulrahman et al. [19] in the existence of convection. According to their research, the exponential profile caused the highest surface temperature under conditions of surface wetness when compared to the temperature distribution of rectangularly shaped fins. Jagadeesha et al. [20] considered the hyperbolic and rectangular shape of the annular fin to explicate the behavior of the heat exchange mechanism within the extended surface. According to their research, the rate at which heat is transmitted is greater for hyperbolic annular fins than for rectangular fins.

In air conditioning and refrigeration management systems, fin-and-tube heat exchangers are crucial elements. Fin-and-tube heat exchangers' system productivity is frequently enhanced by using surfaces with increased surface area. As a result, a variety of enhanced heat transfer surfaces have been devised to strengthen the performance of air-side heat exchange. One of the most common surfaces used in heat exchangers is the wavy fins because they can extend the stream path and disrupt the air movement without significantly increasing pressure drop. The functioning of airside heat exchange with wavy fin-and-tube heat exchangers has been extensively studied using experimental or computational methods. Altun and Ziylan [21] debriefed the natural convective heat transmission through a wavy-finned plate and concluded that more heat was transferred with sinusoidal wavy fins than rectangular fins. Luo et al. [22] studied the impact of diverse corrugation angles on the wavy fin. According to their findings, the heat transmission performance appears to be improved by using innovative wavy fins. Song et al. [23] discussed the heat transmission rate of a heat exchanger with wavy fins. The artificial neural network (ANN) has recently gained popularity as an appealing mathematical technique for examining a variety of physical phenomena models. ANN is a multi-networked (multilayer perceptron) framework of logically organized primary components replicating neuron operation in the human brain. Compared to traditional regression and statistical models, it is more sophisticated and productive. It can model complex and non-linear relationships without making any prior presumptions about the cause-and-effect relationships of the variables. The ANN model is comprised of simple attributes that work together in parallel. Even though each neuron's computational potential is minimal, the parallel operations of many neurons allow the network to perform a wide range of tasks quickly and with various functions. This method was designed to establish structure characteristics while reducing computation time. Predictions from ANNs can be quickly derived with a timeframe on the level of milliseconds once they have been built, which is one of their benefits. An additional benefit of ANNs is that no comprehensive overview of basic concepts is required. The ANN has been employed as a substitute approach in large-scale interpretation to replace time-consuming computational modeling, such as finite element method (FEM) calculations, because of this beneficial property of ANN. Researchers have recently discussed the predicted Artificial Neural Network (ANN) approaches to explain the different models. Pichi et al. [24] utilized the concept of ANN to present the model representing the triangular cavity flow. ANN was used by Alsaiari et al. [25] to estimate the water productivity of diverse strategies of solar stills. Kamsuwan et al. [26] explored the nanoliquid stream in the micro-channel heat exchangers by developing the model with the help of ANN. They employed embedded ANN for nanofluid aspects and regression for water characteristics on the CFD to make the simulation results more realistic. As a consequence, ANN was discovered to be effective in

this regard. The ANN model was provided by Jerry et al. [27] to assess the transfer of heat in the heat exchanger with nanoliquid. The ANN approaches established in their research are beneficial for forecasting heat exchangers' Nusselt number and entropy generation. It was determined that the provided approaches might be employed perfectly rather than further computations. Using ANN, Mehmandousti and Kowsary [28] probed the temperature difference in lithium-ion batteries in the presence of pulsating flow.

Increasing the thermal performance of engineering devices by using various fin types, such as annular fins, porous fins, longitudinal trapezoidal fins, and longitudinal rectangular fins, has undeniably been the subject of numerous investigations. In general, most of the study focused on scrutinizing the thermal distribution in simple and conventional fins. Furthermore, most of the research works were based on the experimental investigation of the heat transfer of fin-and-tube and plate-fin heat exchangers with wavy fins [29–34]. However, the studies of Sertel and Bilen [35] and Khaled [36] discuss the various types of wavy fins to recognize the thermal augmentation attributes. In particular, Khaled [36] studied the thermal variation in the wavy fin with constant thermal conductivity. It is noticed that the thermal conductivity of the fins would remain constant for problems involving conventional fins. Nevertheless, the thermal conductivity is temperature-dependent if there is a significant temperature difference within the fin. Furthermore, these observations indicate that thermal conductivity is temperature-dependent for numerous applications in the engineering domain. As a result, when exploring the fin in such scenarios, the implications of temperature-dependent thermal features must be addressed. This kind of assessment offers a more precise understanding of the wavy fin's thermal performance. Thus, this research is proposed to fill the research gap in determining the thermal response of wavy fins under the impact of various convective mechanisms by considering temperature-dependent thermal conductivity as well as the coefficient of convective heat transfer. In light of the aforementioned communications survey, the thermal response and heat transmission factors in a wavy-structured fin with the effect of convection are investigated in this study by considering the linearly temperature-dependent thermal conductivity and nonlinearly temperature-dependent coefficient of convective heat transfer. The current model is established as ordinary differential equations (ODEs), which can be transformed into dimensionless representations using appropriate similarity transformations. The resulting equation is solved using the RK45 method, and the heat transfer model of a wavy fin is predicted with the aid of an artificial neural network (ANN). The objectives of the present scrutiny are:

- Inspection of thermal variations and heat transfer rates in the wavy fin.
- Determining the thermal distribution in the wavy fin by considering temperature-dependent thermal conductivity and heat transfer coefficient.
- Study of various heat transfer mechanisms in the wavy fin.
- Applying stochastic ANN to analyze the heat transfer rate in the wavy fin.
- The amount of heat transported and the temperature developed within the fin is determined using the ANSYS simulation scheme.

2. Formulation of the Problem

The steady-state temperature performance and heat transmission of a wavy structured rectangular fin with width W and height $2H$, which transmits heat via convection at T_∞ to the environment, are explored in this study. The following basic assumptions are employed in the current study [37,38]:

- Heat conduction in the fin is considered to be a steady state.
- Fin is assumed to transfer heat from its surface via convection.
- The thickness of the wavy fin is so smaller relative to its width that heat transmission from adjacent surfaces may be ignored.
- Coefficient of convective heat transfer and thermal conductivity are taken to be temperature-dependent.
- The fin profile surface is considered to be wavy along the extension axis (x -axis).

- The base temperature of the wavy fin is considered to be uniform.
- The fin’s surrounding is at a uniform temperature.
- It is assumed that the fin tip is adiabatic.
- There is no heat production within the fin.

The corresponding geometrical representation of the wavy fin is revealed in Figure 1, and using the aforesaid assumptions, the equation governing the fin problem is specified by (see Khaled [36]):

$$\frac{d}{dx} \left[K(T) \frac{dT}{dx} \right] = \left[\frac{dA_{SF}}{dx} \right] \frac{h^*(T)}{A_{CS}} (T - T_{\infty}) - \left[\frac{K(T)}{A_{CS}} \frac{dA_{CS}}{dx} \right] \frac{dT}{dx} \tag{1}$$

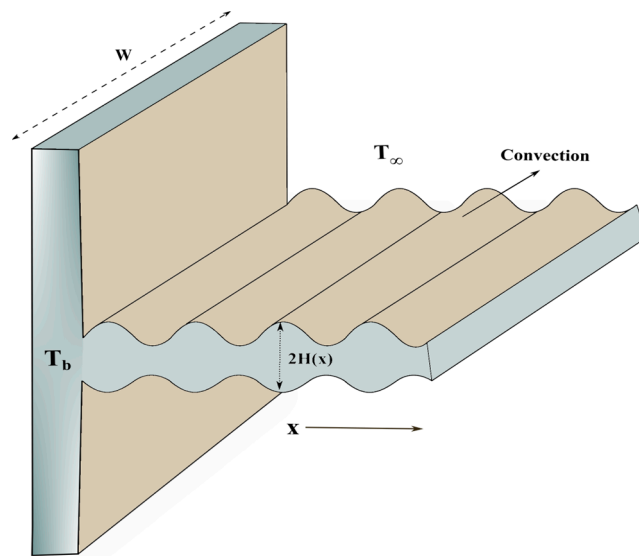


Figure 1. Schematic illustration of a wavy fin.

The first term on the left-hand side refers to conduction, and the convective mechanism is represented by the first term on the right-hand side.

In the above equation, $K(T)$ is the thermal conductivity of the wavy fin material and $h^*(T)$ indicates the coefficient of heat transfer, which are given as:

$$K(T) = k_{\infty} [1 + \chi(T - T_{\infty})],$$

$$h^*(T) = h_b \left(\frac{T - T_{\infty}}{T_b - T_{\infty}} \right)^m \tag{2}$$

Here χ is the slope of the thermal conductivity–temperature curve and m denotes the parameter of heat transfer coefficient. In the majority of applications, m could fall around the range of -3 and 3 and generally can vary between -6.6 and 5 . Furthermore, the different mechanisms of convective heat transfer, including laminar natural convection ($m = 1/4$), turbulent natural convection ($m = 1/3$), nucleate boiling ($m = 2$), and radiation heat transfer ($m = 3$) are all described by this parameter.

From Equations (1) and (2) yields:

$$\frac{d}{dx} \left[k_{\infty} [1 + \chi(T - T_{\infty})] \frac{dT}{dx} \right] + k_{\infty} [1 + \chi(T - T_{\infty})] \frac{dT}{dx} \left[\frac{1}{A_{CS}} \frac{dA_{CS}}{dx} \right] - \frac{1}{A_{CS}} \left[\frac{dA_{SF}}{dx} \right] \frac{h_b (T - T_{\infty})^{m+1}}{(T_b - T_{\infty})^m} = 0, \tag{3}$$

In the above equation, A_{CS} and A_{SF} indicate the cross-sectional area and surface area of the fin, which are mathematically denoted by:

$$A_{CS} = 2H_0 \int_0^W \left\{ 1 + \delta \sin \left[2\pi n \left(\frac{x}{L} \right) + \varphi \right] \right\} dz. \tag{4}$$

and

$$\begin{aligned} A_{SF} &= 2WL_{ta} \\ &= 2W \int_0^L \sqrt{1 + \left(\frac{dH}{dx} \right)^2} dx. \end{aligned} \tag{5}$$

where,

$$L_{ta} = \int_0^L \sqrt{1 + \left(\frac{dH}{dx} \right)^2} dx \text{ and } H = H_0 \left\{ 1 + \delta \sin \left[2\pi n \left(\frac{x}{L} \right) + \varphi \right] \right\}. \tag{6}$$

The associated boundary conditions (BCs) are:

$$x = 0 : T = T_b,$$

$$x = L : \frac{dT}{dx} = 0. \tag{7}$$

Using the respective dimensionless terms, non-dimensionalization is carried out:

$$\Theta = \frac{T - T_\infty}{T_b - T_\infty}, X = \frac{x}{L}, \beta = \chi(T_b - T_\infty), Nc = \frac{h_b L^2}{k_\infty H_0}, a_{RL} = \frac{H_0}{L}. \tag{8}$$

The following dimensionless non-linear differential equation is achieved using the aforementioned dimensionless variables:

$$\begin{aligned} \frac{d}{dX} \left[(1 + \beta\Theta) \frac{d\Theta}{dX} \right] + (1 + \beta\Theta) \left[\frac{2\pi\delta n \cos(2\pi n X + \varphi)}{1 + \delta \sin(2\pi n X + \varphi)} \right] \frac{d\Theta}{dX} - \\ Nc \left[\frac{\sqrt{1 + 4(\pi a_{RL} \delta n)^2 \cos^2(2\pi n X + \varphi)}}{1 + \delta \sin(2\pi n X)} \right] \Theta^{m+1} = 0. \end{aligned} \tag{9}$$

In Equation (9), β (thermal conductivity parameter), Θ (temperature profile), a_{RL} (fin profile aspect ratio) and Nc (convective-conductive parameter) are the non-dimensional terms as defined in Equation (8). Also, δ is the surface wave dimensionless amplitude, n indicates the number of surface waves per fin surface, and φ signifies the surface wave phase shift.

Correspondingly, Equation (7) is reduced as:

$$\begin{aligned} X = 0 : \Theta = 1, \\ X = 1 : \Theta' = 0. \end{aligned} \tag{10}$$

The heat transfer through the wavy fin can be determined by using Fourier's law at the fin's base, and it is described as:

$$q = -K(T) \left[\int_0^W H(x = 0, z) dz \right] \frac{dT}{dx} \Big|_{x=0}. \tag{11}$$

From Equations (2) and (11) yields,

$$q = -k_\infty [1 + \chi(T - T_\infty)] W H_0 \frac{dT}{dx} \Big|_{x=0}. \tag{12}$$

The dimensionless expression of Equation (12) is referred to as:

$$Q = \frac{q}{k_{\infty}(T_b - T_{\infty})W'} \\ = -[1 + \beta\Theta(0)] a_{RL} \left. \frac{d\Theta}{dX} \right|_{X=0}. \quad (13)$$

3. Network Configuration and Design of ANN

Artificial neural networks use a network of interconnected “neurons” to accomplish sophisticated modeling of input data to an output function. A multilayer perceptron network model is trained in the current study to predict the results of the heat transfer analysis of the wavy fin. An ANN is a three-layer (input, hidden, and output layers) feedforward neural network architecture [39,40]. An input layer is composed of many neurons. Similar to an established regression scheme, each neuron symbolizes an independent variable. The entire number of neurons in the input layer equals the number of independent variables. The neurons in the input layer will connect to those in the hidden layer. The hidden layer is then developed to govern the input neurons, forecast the responses of the output neurons, and represent signals using the activation function.

The mathematical representation of ANNs can be expressed as

$$a = \sum_{j=0}^N \omega_j \zeta_j + B_0$$

where N represents the number of inputs, B_0 and ω_j denote the bias and weight, and ζ_j indicates the input value.

The iterative operation of acquiring a solution to the problem is executed by training and testing the neural network with training algorithms. The Levenberg–Marquardt (LM) optimization technique is implemented for training the ANN for the proposed fin problem. The LM procedure is a form of supervised training approach that may be utilized with any feedforward neural network. The LM algorithm has been employed for curve fitting because it incorporates the feature of superior convergence of the Gauss–Newton approach near the minima with the lowering level of error attained by gradient descent. The LM algorithm’s (LMA) fundamental principle is to execute incorporated process training in and around a region with a complicated curvature. To develop a quadratic strategy, the LMA initially employs the steepest descent procedure. The LMA transforms to the Gauss–Newton technique for substantially speeding out convergence. In order to train the network, the input and output layers are loaded with the inputs and their corresponding outputs. The first step in developing an NN-BLMA model is effectively choosing the input and output data. The model should accurately represent the heat transfer of the fin without transferring duplicative or unnecessary parameters. The significant thermal parameters, such as thermal conductivity and convective-conductive parameter values for various magnitudes of m are chosen as input data and heat transfer values are taken as target data for analyzing the heat transfer performance of the fin. The scenarios and cases that illustrate the fin problem are provided in Table 1.

Table 1. Details of scenario and cases for NN-BLMA of the wavy fin.

Scenario	Case	Parameters	
		β	N_c
m = 1/4	1	-1	1
		-0.5	1
		0	1
		0.5	1
		1	1
	2	1.5	1
		0.6	0
		0.6	0.1
		0.6	0.5
		0.6	0.7
m = 1/3	1	0.6	0.9
		0.6	1
		-0.6	0.5
		-0.4	0.5
		0	0.5
	2	0.4	0.5
		0.6	0.5
		0.8	0.5
		0.7	0
		0.7	1
m = 2	1	0.7	1.5
		0.7	2
		0.7	2.5
		0.7	3
		-0.2	2
	2	0	2
		0.2	2
		0.4	2
		0.6	2
		0.8	2
	2	0.4	1
		0.4	1.1
		0.4	1.2
		0.4	1.3
		0.4	1.4
		0.4	1.5

Table 1. Cont.

Scenario	Case	Parameters	
		β	Nc
m = 3	1	0.1	0.2
		0.3	0.2
		0.5	0.2
		0.7	0.2
		0.9	0.2
		1	0.2
	2	0.3	1
		0.3	1.2
		0.3	1.4
		0.3	1.6
		0.3	1.8
		0.3	2.0

The transfer functions for neurons in the hidden layer and the output layers are referred to as PURELIN and TANSIG, respectively, in the training phase and are given as:

$$f(x) = \text{purlin}(x) = x,$$

$$f(x) = \text{tansig}(x) = \frac{2}{(1 + e^{-2x})} - 1.$$

The mathematical notations for the Mean Squared Error (MSE), coefficient of determination (R^2), and the Error rate of networks are indicated as follows:

$$MSE = \frac{1}{j} \sum_{i=1}^j \left(\Theta_{RKF-45(i)} - \Theta_{ANN(i)} \right)^2,$$

$$R^2 = 1 - \left[\frac{\sum_{i=1}^j \left(\Theta_{RKF-45(i)} - \Theta_{ANN(i)} \right)^2}{\sum_{i=1}^j \left(\Theta_{RKF-45(i)} \right)^2} \right],$$

$$\text{Errorrate}(\%) = \left[\frac{\Theta_{RKF-45(i)} - \Theta_{RKF-45(i)}}{\Theta_{RKF-45(i)}} \right] \times 100.$$

4. Validation of the Model

The proposed fin model is validated for authenticity by comparing it to the wavy fin model presented in [36]. The heat transfer performance for various types of wavy fins is also examined in the available literature [36], which can be adopted to analyze the thermal distribution and heat transfer rate through wavy fins in the present study. The following governing equation for the fin problem is presented by Khaled [36]:

$$\frac{d}{dx} \left[K \frac{dT}{dx} \right] = \left[\frac{dA_{SF}}{dx} \right] \frac{h^*}{A_{CS}} (T - T_{\infty}) - \left[\frac{K}{A_{CS}} \frac{dA_{CS}}{dx} \right] \frac{dT}{dx} \tag{14}$$

with constant thermal conductivity and the coefficient of heat transfer, and where

$$A_{CS} = 2H(x)W, \text{ and } A_{SF} = 2W \int_0^L \sqrt{1 + \left(\frac{dH}{dx}\right)^2} dx. \tag{15}$$

Equation (14) is transformed using Equation (8) to yield the corresponding dimensionless equation. In other words, the developed dimensionless energy equation (Equation (9)) of the current investigation can be transformed into the dimensionless wavy fin model of [36] for some reduced cases ($\beta = 0$ and $m = 0$), which is presented as follows:

$$Nc \left[\frac{d^2\Theta}{dX^2} + \left[\frac{2\pi\delta n \cos(2\pi nX + \varphi)}{1 + \delta \sin(2\pi nX + \varphi)} \right] \frac{d\Theta}{dX} - \frac{\sqrt{1 + 4(\pi a_{RL} \delta n)^2 \cos^2(2\pi nX + \varphi)}}{1 + \delta \sin(2\pi nX)} \right] \Theta = 0. \tag{16}$$

where $Nc = \frac{h^*L^2}{KH_0}$ denotes the non-dimensional convective-conductive parameter with constant thermal conductivity and the coefficient of heat transfer.

The above equation indicates the governing heat equation of the wavy fin with constant thermal conductivity and heat transfer coefficient, similar to Case A’s problem in [36]. The detailed procedure for achieving the solution of the corresponding equations of the wavy fin is described in [36]. Furthermore, the comparison between the current study results and Khaled’s [36] work on the fin model is performed and is exhibited in Table 2. The tabulated values in this table indicate the temperature profile results at the wavy fin’s tip. The table highlights that the NN-BLMA solutions estimated in the present analysis and the solution of Khaled [36] have an excellent agreement for the given cases of $Nc (= 0.25, 1.00, 2.25, 4.00)$ with $\beta = 0, a_{RL} = 0, \delta = 0,$ and $n = 2$. This comparison scrutiny includes an error analysis of the results, with a maximum error of 0.03% and an average error of 0.00091275%. Additionally, the ANN and RKF-45 results for the heat flux of the wavy fin are compared in Table 3 by varying β and Nc . The tabulated results indicate that the ANN and RKF-45 numerical results are in good accordance. The numerical results in these tables support the reliability of the proposed wavy fin model.

Table 2. Validation of the present fin problem with the research work of [36] for $\beta = 0, a_{RL} = 0, \delta = 0,$ and $n = 2$.

Nc	$\Theta(1)$			
	Khaled [36]	RKF-45	NN-BLMA	Error %
0.25	0.886819	0.886818903534562	0.886818678821468	3.6×10^{-5}
1.00	0.648054	0.648054498479555	0.648073326471297	3.0×10^{-3}
2.25	0.425096	0.425096032263199	0.425093687869883	5.4×10^{-4}
4.00	0.265802	0.265802207758634	0.265802198782017	7.5×10^{-5}

Table 3. NN-BLMA and RKF-45 results of Q for varying β and Nc .

β	Nc	Q	
		RKF-45	NN-BLMA
0.5		0.81519713	0.815209440
0.51		0.81104380	0.811030034

Table 3. Cont.

β	N_c	Q	
		RKF-45	NN-BLMA
0.52		0.80693640	0.806919268
0.53		0.80287422	0.802864308
0.54		0.79885639	0.798856272
0.55		0.79488212	0.794889631
	1	0.70773327	0.707742900
	1.02	0.71847530	0.718451779
	1.04	0.72912124	0.729114349
	1.06	0.73967263	0.739685472
	1.08	0.75013112	0.750148337
	1.1	0.76049809	0.760505472

The numerical results of the wavy fin indicating its thermal profile values at different $X (= 0, 0.2, 0.4, 0.6, 0.8, 1)$ are presented in Table 4 with the varying magnitude of β and m . It is evident from this table that the magnitude of the thermal profile increases in accordance with an increase of $\beta (= -0.5, 0.0, 0.5)$ for all the considered cases of $m (= 1/4, 1/3, 2, 3)$. In precise, the highest temperature profile values are observed for $\beta > 0$, and $\Theta(X)$ value is minimum for $\beta < 0$. The numerical solution for the fin governing equation (Equation (9)) is achieved for the constant thermal conductivity parameter ($\beta = 0$). The thermal profile values for $\beta = 0$ are much higher than the results of $\beta < 0$ and are lesser than the results of $\beta > 0$. This occurs because the fin’s capacity to transfer heat strengthens with an improvement in the thermal conductivity gradient, which elevates the temperature. Moreover, the m parameter represents the fin’s heat convection behavior; when the m parameter rises, the temperature profile increases, indicating that the fin is performing better.

Table 4. Numerical results of $\Theta(X)$ for various cases of β and m at $\varphi = 0, a_{RL} = 0.1, \delta = 0.1,$ and $n = 2$.

		X						
		β	0	0.2	0.4	0.6	0.8	1
$\Theta(X)$	$m = \frac{1}{4}$	-0.5	1.0000	0.81501	0.68675	0.60976	0.56980	0.55512
		0.0	1.0000	0.88041	0.78270	0.71808	0.68271	0.66939
		0.5	1.0000	0.91147	0.83576	0.78395	0.75495	0.74391
	$m = \frac{1}{3}$	-0.5	1.0000	0.81841	0.69271	0.61733	0.57823	0.56387
		0.0	1.0000	0.88222	0.78626	0.72292	0.68829	0.67526
		0.5	1.0000	0.91257	0.83801	0.78708	0.75860	0.74777
	$m = 2$	-0.5	1.0000	0.86191	0.76912	0.71427	0.68606	0.67573
		0.0	1.0000	0.90657	0.83380	0.78705	0.76189	0.75250
		0.5	1.0000	0.92822	0.86953	0.83056	0.80916	0.80109
	$m = 3$	-0.5	1.0000	0.87691	0.79545	0.74761	0.72308	0.71411
		0.0	1.0000	0.91545	0.85092	0.80993	0.78802	0.77986
		0.5	1.0000	0.93427	0.88154	0.84695	0.82809	0.82100

5. Results and Discussion

5.1. Thermal and Heat Transfer Analysis

This portion explicates the mathematical analysis of the proposed fin problem in detail using graphs and tables. In more aspects, the physical properties of thermal factors, including the convective-conductive parameter and thermal conductivity parameter on thermal profile quantities with regard to thermal variation in the wavy fin, are carried out. These findings are well explained and graphically presented in the figures by comparing them to the rectangular fin. The solid lines in these graphs portray wavy fin behavior, while the dashed lines represent rectangular fin behavior. Moreover, the significance of physical parameters such as convective-conductive parameter and thermal conductivity parameter on the heat transfer of the wavy fin is comprehensively researched using NN-BLMA. Figure 2 displays the performance of Θ with the consequence of β at $\varphi = 0$, $a_{RL} = 0.2$, $\delta = 0.2$, $Nc = 0.3$, and $n = 4$. It shows that Θ increases with an upsurge in β magnitude. The heat conduction through the fin is strengthened by increased levels of the thermal conductivity parameter, which raises the temperature of the fin as an effect. It is worth highlighting that $\beta = 0$ indicates the constant thermal conductivity provided by k_∞ . Curves with $\beta > 0$, as seen in this figure, relate to fin materials whose thermal conductivity rises as temperature rises from T_a to T_b . The same nature of the temperature profile curve can be seen for $\beta < 0$. Additionally, it signifies that the temperature profile curves of the wavy fin are below the rectangular fin curves.

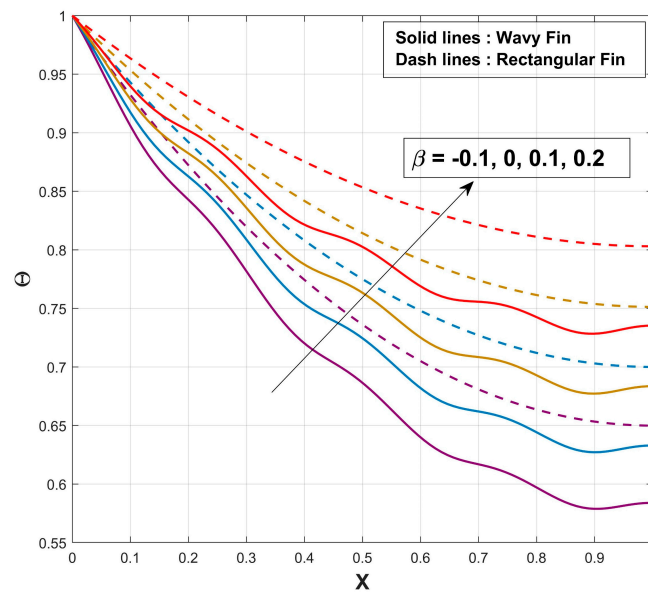


Figure 2. Impact of β on Θ of wavy and rectangular profiled fin.

Figure 3 portrays the nature of Θ against Nc with $\varphi = 0$, $a_{RL} = 0.2$, $\delta = 0.2$, $\beta = 0.1$, and $n = 4$. It depicts that Θ decreases as Nc increases, and the temperature distribution of the wavy fin is lesser than the temperature distribution of the rectangular fin. Referring to the graph, increasing this parameter magnitude elevates the rate of convective heat transferring through the wavy fin as the overall temperature falls more rapidly. Figure 4 indicates the features of Θ with the impact of n by taking $\varphi = 0$, $a_{RL} = 0.2$, $\delta = 0.2$, $Nc = 0.15$, and $\beta = 0.4$. This figure displays that Θ decreases as the number of waves of the wavy fin increases at $Nc = 0.15$. Figures 5–7 also show that Θ decreases as the number of waves increases at $Nc = 0.20$, 0.25 , and 0.30 , respectively, with $\varphi = 0$, $a_{RL} = 0.2$, $\delta = 0.2$, and $\beta = 0.3$. This is due to the fact that higher n values lead to greater oscillation in the cross-sectional area of the wavy fin within its differential segments. Therefore, as n progresses, conduction via the fin can asymptotically approximate conduction through the average area of the cross-section. Figure 8 depicts the characteristics of Θ with the

impact of a_{RL} at $\varphi = 0, \delta = 0.3, \beta = 0.4,$ and $Nc = 0.3$. It conveys that Θ decreases as a_{RL} increases at $n = 2$. With the observation of Figures 4–8, it is obvious that the wave structure of temperature curves becomes steeper. Figures 9 and 10 also display the nature of Θ versus a_{RL} at $n = 3$ and $n = 4$ with $\varphi = 0, \delta = 0.3, \beta = 0.4,$ and $Nc = 0.3$. They show that Θ decreases as a_{RL} increases at $n = 3,$ and $n = 4,$ respectively. The temperature curves of these figures display that the temperature profile decreases as the number of waves per fin surface increases. The different kinds of heat transport in the wavy fin are discussed graphically, and Figure 11 displays the implications of m on the non-dimensional temperature profile of the fin by considering $\varphi = 0, a_{RL} = 0.2, \delta = 0.2, \beta = 0.1, Nc = 0.2,$ and $n = 6$. A greater amount of heat diffuses from the fin when the m value is decreased, transferring energy more effectively. It is implied that the fin’s performance increases as the m parameter diminishes.

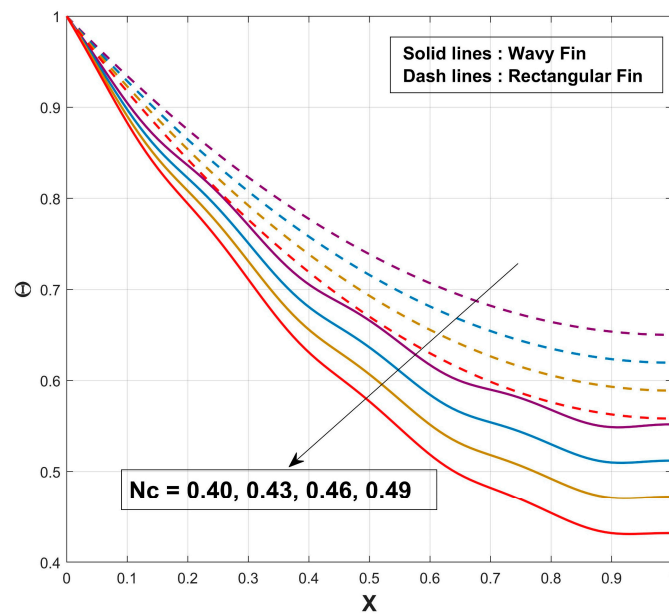


Figure 3. Impact of Nc on Θ of wavy and rectangular profiled fin.

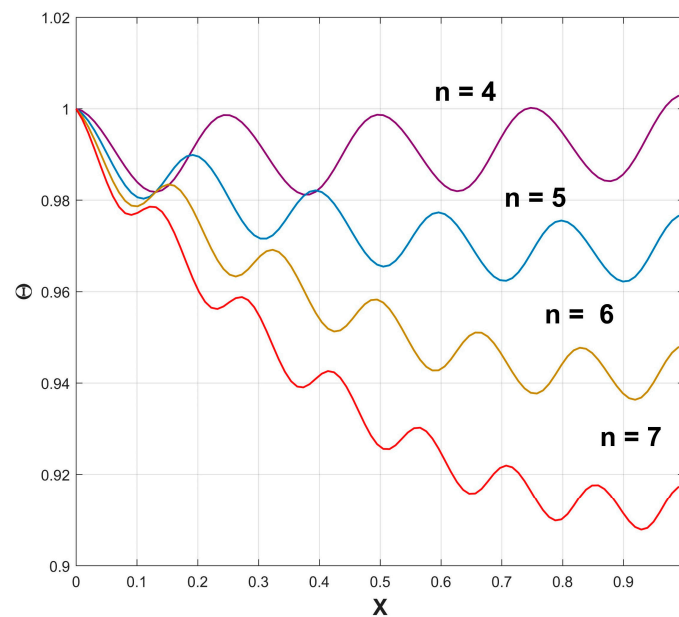


Figure 4. Impact of n on Θ of wavy profiled fin for $Nc = 0.15$.

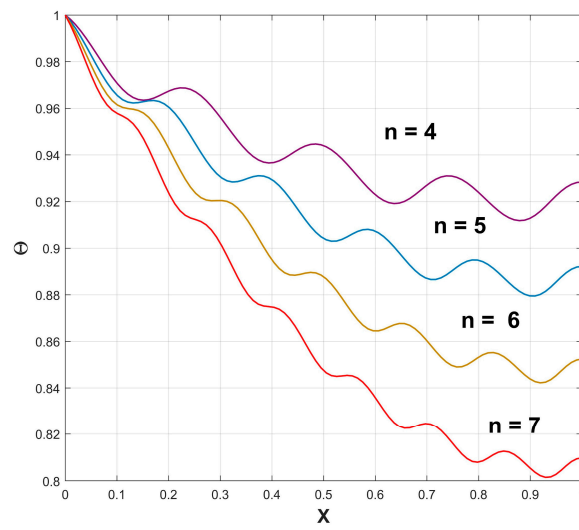


Figure 5. Impact of n on Θ of wavy profiled fin for $Nc = 0.20$.

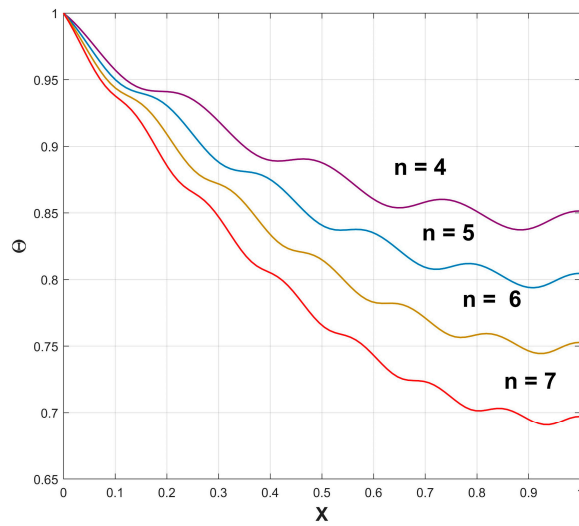


Figure 6. Impact of n on Θ of wavy profiled fin for $Nc = 0.25$.

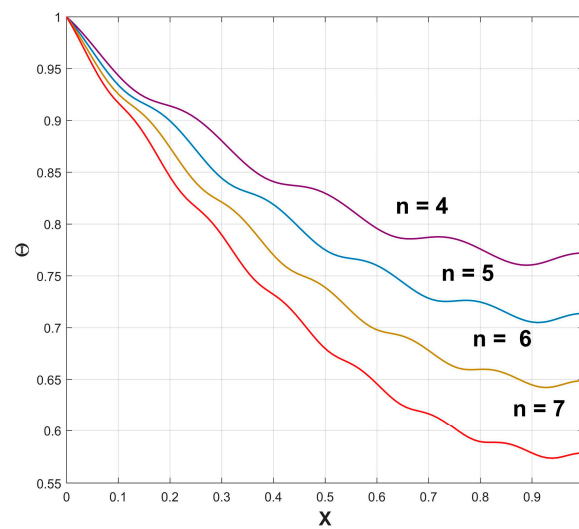


Figure 7. Impact of n on Θ of wavy profiled fin for $Nc = 0.30$.

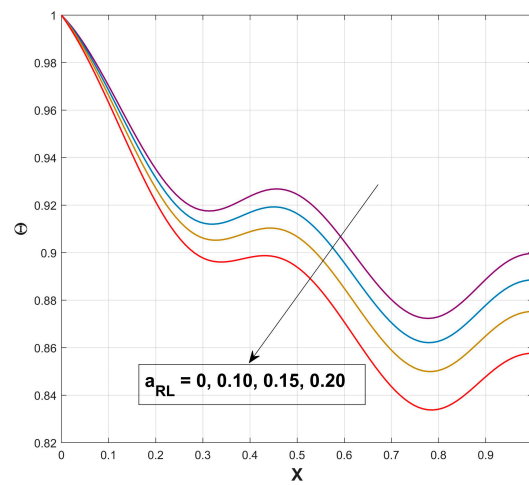


Figure 8. Impact of a_{RL} on Θ of wavy profiled fin for $n = 2$.

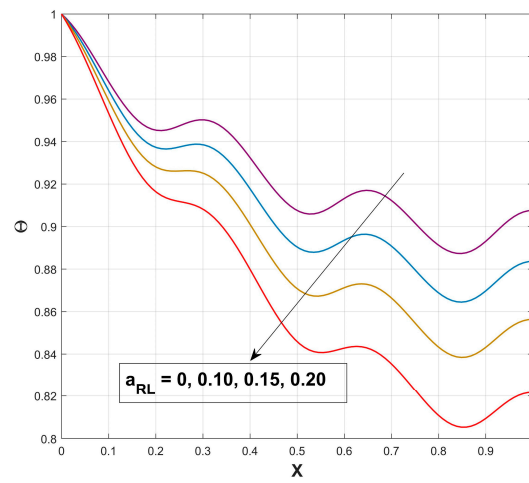


Figure 9. Impact of a_{RL} on Θ of wavy profiled fin for $n = 3$.

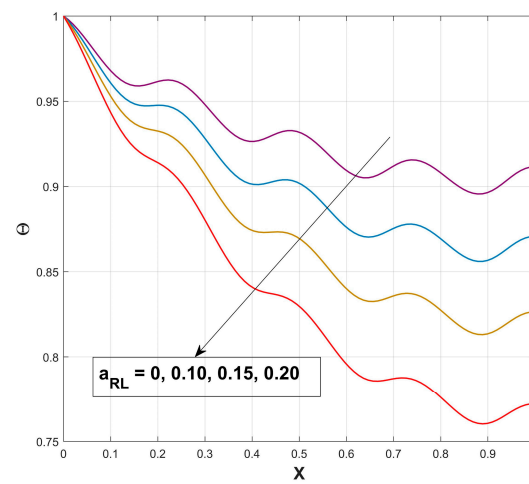


Figure 10. Impact of a_{RL} on Θ of wavy profiled fin for $n = 4$.

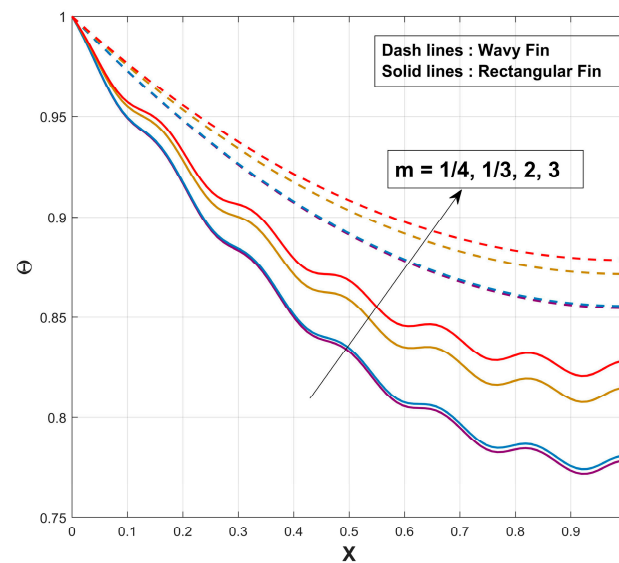


Figure 11. Impact of m on Θ of wavy and rectangular profiled fin.

5.2. Thermal and Heat Transfer Analysis Using ANN

ANN is a computational model inspired by the operational characteristics of biological neural networks. ANN assigns information among the weight coefficients of the connection in the multilayer perceptron network (MPN) design to increase the network's fault tolerance and robustness. Assessing the impact of each input parameter on the output variable is an important aspect of the ANN algorithm. ANN has the perceptible benefit of being capable of learning automatically from instances, which means that the correlations between input and output coefficients are formed by the data themselves, relieving the researcher's responsibility of determining the suitable regression equation. Another significant feature is its potential for generalization, which allows for the estimation of unknown solutions after a network training technique has been able to interpret the learned information. Additionally, ANNs have the capacity to address complicated problems and can be applied to study mechanical characteristics, heat transfer problems, fracture mechanics, and fatigue. ANN is simple to use and interprets appropriate results compared to statistical techniques. However, ANNs have multiple sets of hyperparameters that need to be tuned, which is a significant limitation. An ANN model using an MPN is established in this study to predict heat transfer in a wavy fin. Figure 13 indicates the structure of the ANN. The ANN model used in this study consists of an input layer, a hidden layer with ten neurons, and an output layer with one neuron. In the input and output layers, every neuron has a corresponding design variable. The validation performance as an MSE indicator is displayed in Figure 13a for the heat flux of the wavy fin. Initially, the MSE level is high and attains the best performance with an increase in the epoch. The optimum value of this trained network reaches 3.0495×10^{-10} at the 141st epoch. It can be spotted from this figure that, as the network is trained, the MSE falls, with epoch 141 having the lowest mean square error. The gradient, μ , and validation checks for heat flux data are given in Figure 13b. The developed model exhibits a gradient of 9.8764×10^{-8} at the 141st epoch indicating the optimal training of the network. The statistical results for the subjected data are in the form of regression analysis, as presented in Figure 13c. It is evident from the figure that the R values for training, testing, and validation are all 1. As a result, the ANN's predicted behavior demonstrated that the heat flux model and the numerical data agreed well. Thus, it is determined that ANN is the most reliable prediction model. The error histogram for the entire procedure is shown in Figure 13d, with emphasis on training, validation, testing, and minimal error. The error histogram shows the blue color model for the training set, red for the testing dataset, and green for the validation dataset. A fine perpendicular line in the orange-colored line indicates the spot on the plot where the error tends to zero. Using the

back-propagation-based algorithm, an error histogram with 20 bins confirmed the test's lowest error of -1.9×10^{-7} . The comparison of RKF-45 and ANN data for the variation in β and N_c is provided in Figure 13e, and Figure 13f, respectively. The results of the heat flux for varied parameters exhibit good accordance. The variation in β causes a decrement in the heat flux while the heat flux increases with an augmentation of N_c . Furthermore, the error between the ANN and RKF-45 data is represented in these figures. The NN-BLMA results of the heat transfer rate data for training, validation, testing, epochs, performance, Mu, and time consumed are displayed in Table 5.

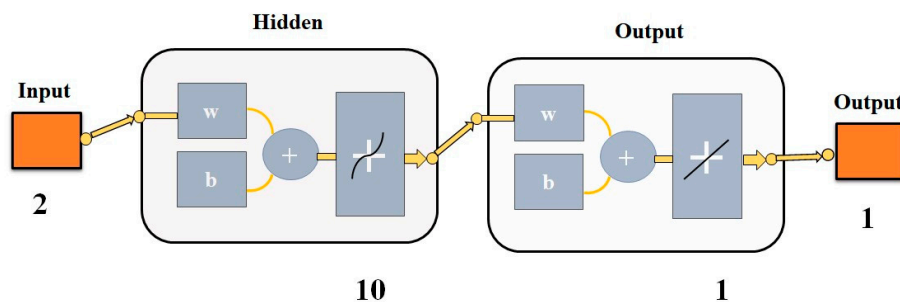


Figure 12. ANN design model.

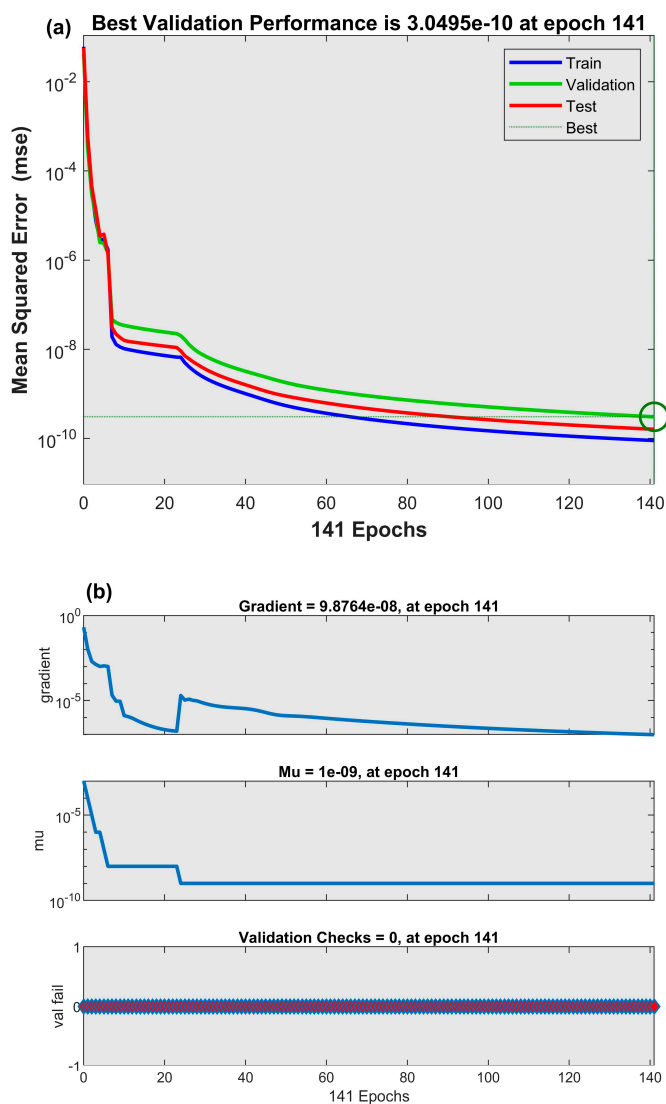


Figure 13. Cont.

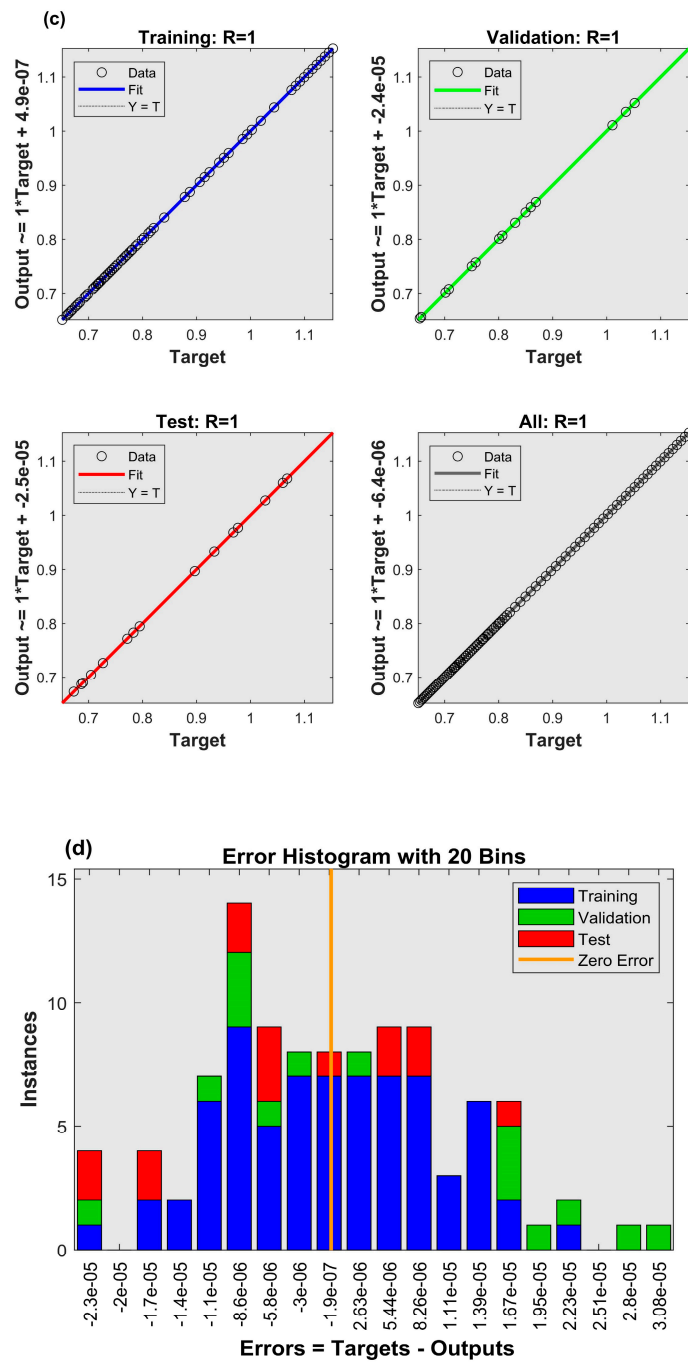


Figure 13. Cont.

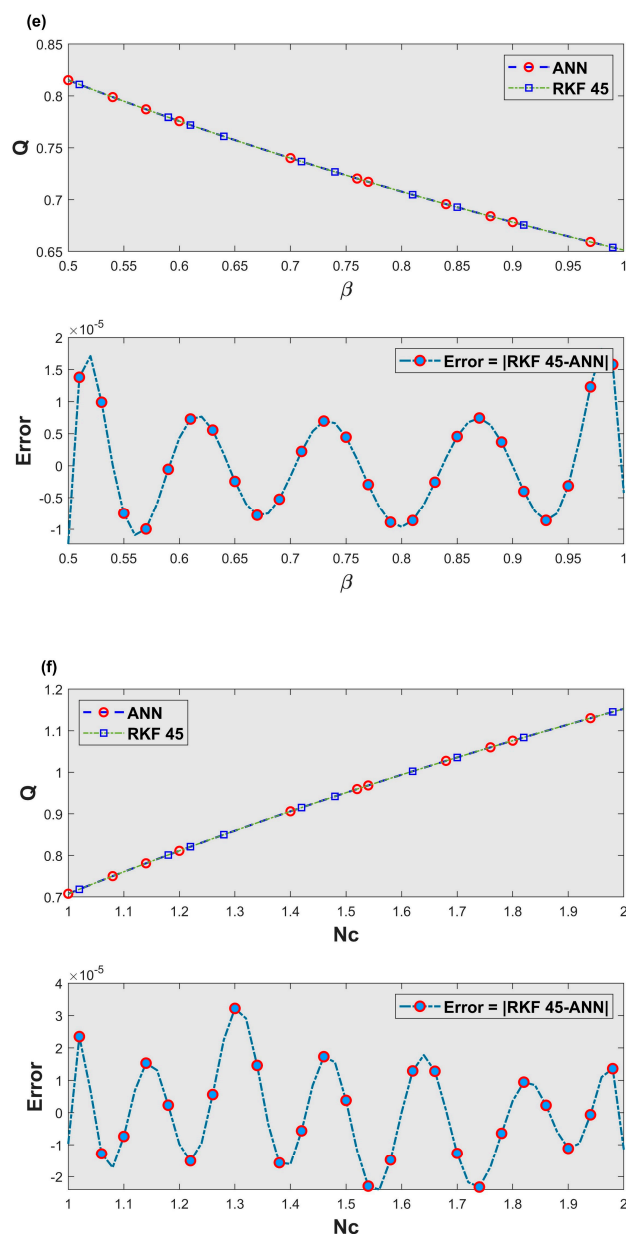


Figure 13. (a) Performance plot. (b) Transition plot. (c) Regression plot. (d) Error histogram plot. (e) Fitness plot of β . (f) Fitness plot of N_c .

Table 5. Results of NN-BLMA for the considered cases of the wavy fin.

Scenario	Case	MSE			Time (s)	Performance	Mu	Grad	Epochs
		Training	Validation	Testing					
m = 1/4	1	2.94×10^{-10}	3.90×10^{-10}	3.52×10^{-9}	1	2.95×10^{-10}	1×10^{-8}	9.74×10^{-8}	88
	2	1.45×10^{-11}	1.54×10^{-11}	2.51×10^{-11}	1	1.45×10^{-11}	1×10^{-10}	9.58×10^{-8}	57
m = 1/3	1	1.42×10^{-11}	3.43×10^{-11}	3.11×10^{-11}	<1	1.42×10^{-10}	1×10^{-10}	9.91×10^{-8}	158
	2	1.92×10^{-10}	1.61×10^{-10}	9.27×10^{-10}	5	1.61×10^{-10}	1×10^{-9}	5.60×10^{-7}	128
m = 2	1	2.09×10^{-12}	5.33×10^{-12}	5.22×10^{-12}	5	2.07×10^{-12}	1×10^{-10}	9.88×10^{-8}	145
	2	1.27×10^{-10}	1.60×10^{-10}	1.51×10^{-11}	5	1.27×10^{-10}	1×10^{-9}	9.80×10^{-8}	99
m = 3	1	4.68×10^{-11}	1.75×10^{-10}	6.96×10^{-11}	3	4.68×10^{-11}	1×10^{-9}	9.85×10^{-8}	244
	2	1.37×10^{-10}	2.54×10^{-10}	2.43×10^{-10}	8	1.30×10^{-10}	1×10^{-9}	2.78×10^{-7}	109

5.3. Thermal and Heat Transfer Analysis Using ANSYS

Thermal analysis determines how much heat is transferred between and within different parts of the device and its surroundings. This is a significant design concern because many components have temperature-dependent characteristics. Another factor to take into account is product security; if an item or equipment is excessively heated, a safety barrier might need to develop over it. Thus, fins are utilized in various engineering applications to improve convective heat exchange and transmit surplus heat from the body to the environment. The surface area exposed to convection and the heat transfer coefficient play a major role in the convective transference of heat. Hence, the steady-state convective thermal analysis has been accomplished using ANSYS 2023 R1 for both rectangular and wavy fins. The software tackles all of the mathematical expressions governing the behavior of these elements, resulting in a thorough explication of how the system functions as an entire unit. Following that, these findings might be displayed graphically. Materials used for fins have major implications for efficient heat transfer and cooling. Aluminium, cast iron, copper, magnesium, and other materials are common fin materials utilized in cooling engines. Since aluminium is a good thermal and electrical conductor, it is used as the primary material of the wavy fin in this study. The aluminium has good corrosion resistance and properties, including thermal conductivity of $237.5 \text{ Wm}^{-1}\text{K}^{-1}$, density of 2689 kgm^{-3} , and specific heat of $951 \text{ Jkg}^{-1}\text{K}^{-1}$ at constant pressure.

The wavy fin's thermal and convective heat transfer analysis is debriefed by comparing it with a rectangular fin. The modeled wavy fin is 15 mm wide and attached to a primary surface of 20 mm high. The three waves per surface are considered, with a total length of 20 mm and thickness of 1 mm. The wavy fin modeling details are displayed in the graphical form in Figure 14. The computational domain for wavy fin has been generated, meshed, and simulated with 7388 elements and 13,639 nodes. Tetrahedral meshing is chosen as the mesh input in the solver to provide better analytical findings. The corresponding meshing analysis is portrayed in Figure 15. The fin tip for the investigation is taken to be adiabatic, and the heat flux of 1000 Wm^{-2} is considered at the primary surface. The surrounding fluid is at a temperature of $T_{\text{surr}} = 325 \text{ K}$, and the value of the convective heat transfer coefficient h^* is $10 \text{ Wm}^{-2}\text{K}^{-1}$. Under these settings, the temperature distribution and heat flux rate have been analyzed for rectangular and wavy aluminium fins depicted in Figures 16 and 17. In Figure 16, it can be observed that the base temperature is 369.83 K and 362.91 K for rectangular and wavy fins. The tip temperature for rectangular and wavy fins are 368.18 K and 361.58 K, respectively. Additionally, the temperature at the middle portion of these fins is about 369.27 K and 362.02 K, respectively. Moreover, as shown in Figure 17, the heat flux is comparatively higher in wavy fins than in rectangular fins.

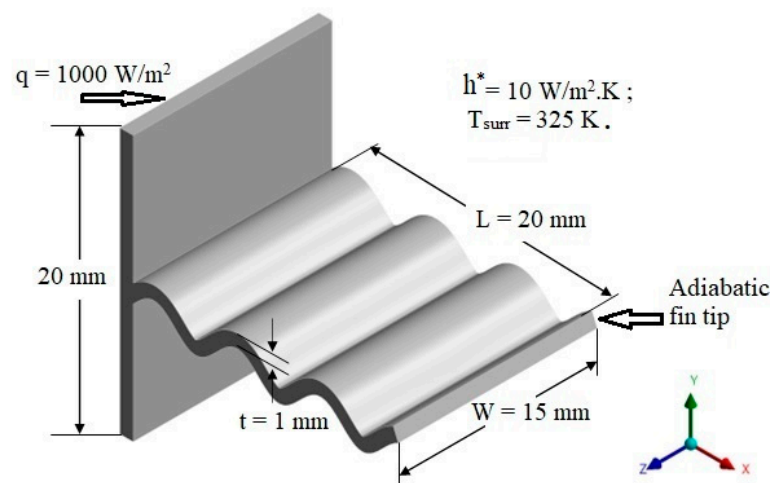


Figure 14. Modeling of the wavy fin.

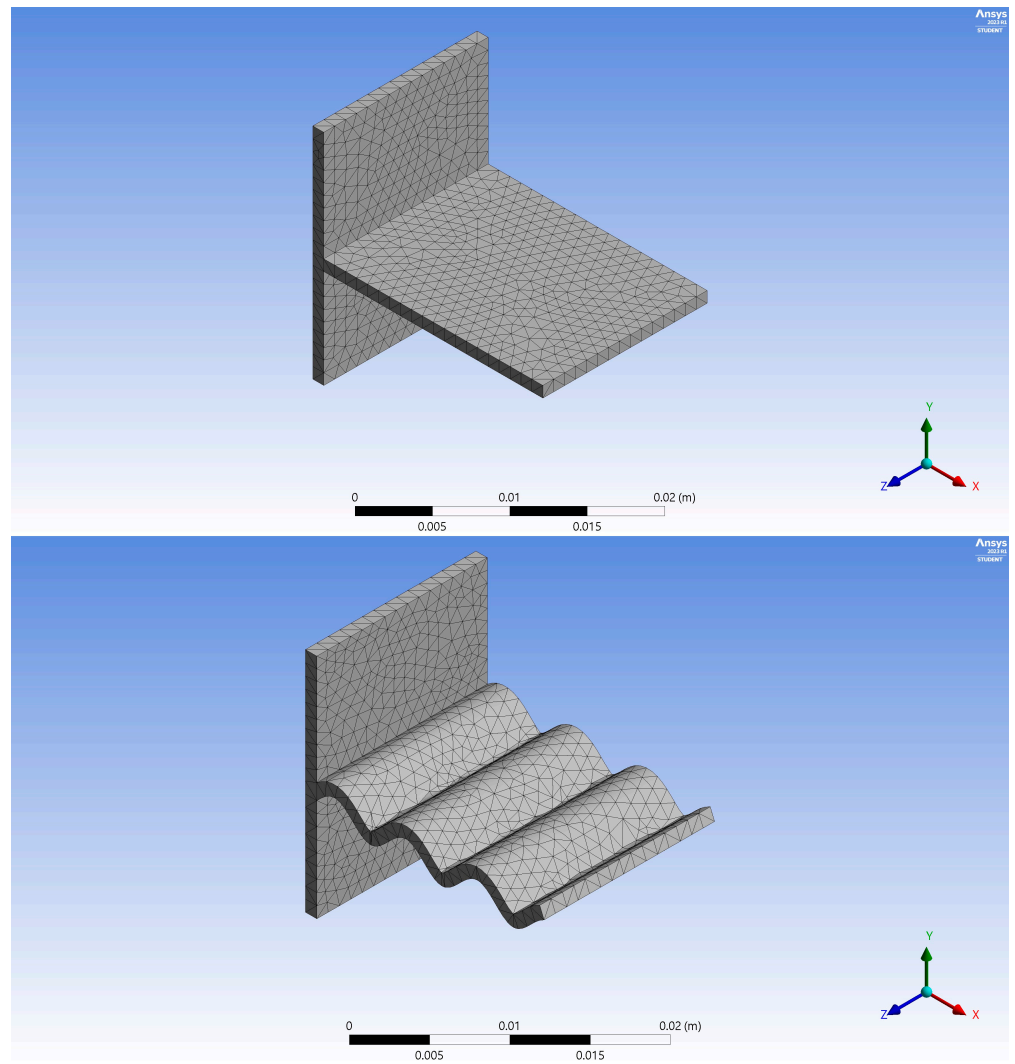


Figure 15. Mesh generation for rectangular and wavy fin.

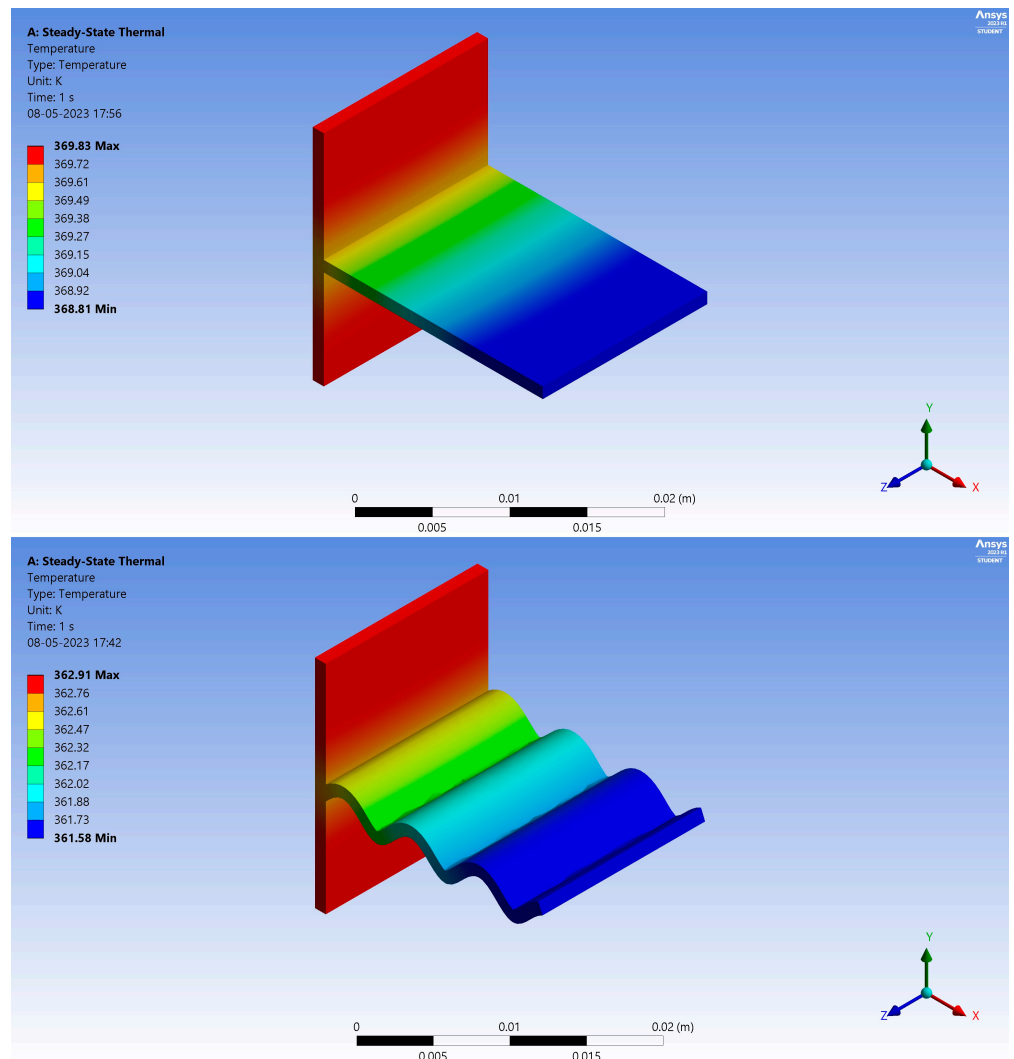


Figure 16. Thermal distribution in rectangular and wavy fin.

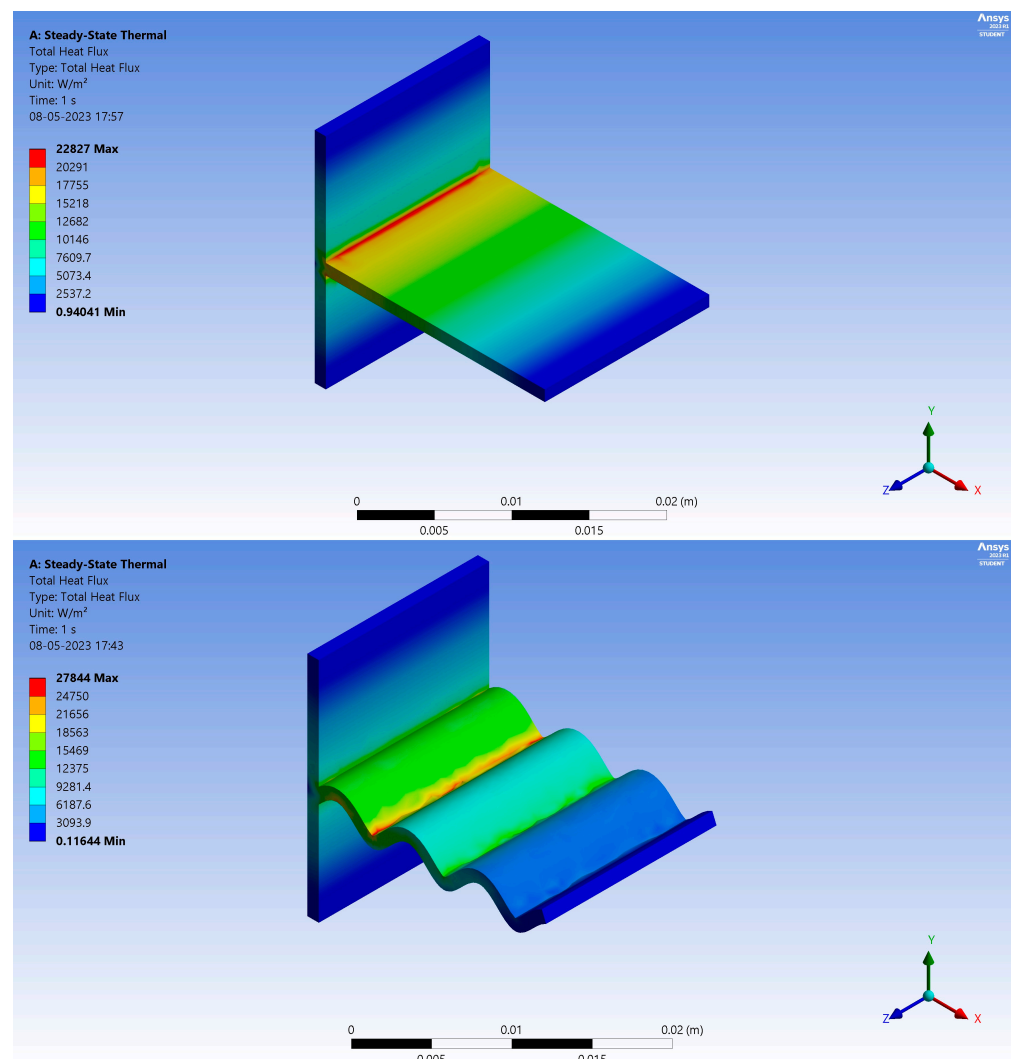


Figure 17. Heat flux variation in rectangular and wavy fin.

6. Conclusions

The thermal distribution in a wavy fin with convective heat transmission is researched. The dimensionless ODE is obtained by introducing similarity transformations to the thermal equation of the wavy fin. Later, the obtained dimensionless differential equations are cracked using the RKF-45 numerical scheme. A mathematical model for the heat transfer analysis of a wavy fin with temperature-dependent thermal conductivity has been developed using Stochastic NN-BLMA. The testing, training, and validation procedures of NN-BLMA and correlation to ensure the proposed model's accuracy assess the estimated solution for various scenarios. Furthermore, the thermal investigation in the wavy fin is performed using the ANSYS simulation scheme. The aforementioned analysis presents the following significant findings:

- The thermal distribution enhances in the wavy fin as the thermal conductivity parameter increases.
- The lesser values of the convective-conductive parameter upsurge the thermal response of the wavy fin.
- As the number of surface waves per fin surface increases, the thermal distribution is reduced.
- An increase in the fin profile aspect ratio causes a decrease in thermal distribution.
- The fin material with a lower thermal conductivity value yields a higher heat transfer rate.

- The rate of heat transfer is more for strong convective heat transfer, which is dependent on the parameter of the convective coefficient as well as the convective-conductive parameter.
- The wavy fins’ performance is assessed by means of surface area, cross-sectional area gradient at the base, and arc length in relation to the regular fin. The thermal distribution is lower for a wavy fin than a rectangular profiled fin; thus, the heat transfer rate is higher for a wavy fin.
- The designed NN-BLMA model has been determined to be credible due to its high consistency during training, validation, and testing.
- The error histograms show very little variation in the error tiers. The performance, regression model, and error histograms’ findings indicate that the training phases of the NN-BLMA models established for determining heat transfer through a wavy fin have been efficiently accomplished.
- The ANSYS simulation results illustrate that the thermal distribution in the rectangular fin is more pronounced than in the wavy fin due to convective heat transfer. As a consequence, the wavy fin transmits heat more effectively.

The adoption of wavy fins in compact fin heat exchangers is noteworthy; these fins were able to improve heat transmission through thermal-hydraulic performance. Therefore, the goal of this study is to examine heat transmission improvements in the wavy fin, which are utilized in the heat exchange system. In this direction, consideration of heat transfer liquids, porous materials, and magnetic impact along with wavy fins can lead to significant improvements in the heat transfer mechanism. However, compared to the heat transfer equations of the ordinary fins, describing the governing mathematical model of the wavy fin and achieving its numerical or analytical solution is quite difficult.

Author Contributions: Conceptualization, G.S.; Methodology, R.S.V.K. and I.E.S.; Validation, M.D.A. and F.G.; Formal analysis, M.D.A.; Investigation, R.S.V.K.; Data curation, F.G.; Writing—original draft, G.S.; Writing—review & editing, I.E.S. All authors have read and agreed to the published version of the manuscript.

Funding: The authors extend their appreciation to the Deanship of Scientific Research at King Khalid University for funding this work through large group Research Project under grant number RGP2/78/44.

Data Availability Statement: Not applicable.

Conflicts of Interest: The authors declare no conflict of interest.

Nomenclature

a_{RL}	Fin profile aspect ratio	φ	Surface wave phase shift
δ	Surface wave dimensionless amplitude	K	Thermal conductivity
Nc	Convection–conduction parameter	H_0	Fin base half height
m	Exponent constant	h^*	Convective heat transfer coefficient
n	Number of surface waves per fin surface	Θ	Non-dimensional temperature
T	Temperature	x	Fin axial distance
A_{CS}	Fin cross-sectional area	β	Thermal conductivity parameter
H	Fin half height	X	Fin’s length (dimensionless)
L	Fin’s length	A_{SF}	Fin surface area
χ	Slope of the thermal conductivity–temperature curve	Subscripts	
W	Width	b	Base
L_{ta}	Wavy fin total arc length	∞	Ambient
q	Heat flux		
Q	Dimensionless heat flux		

References

1. Gorla, R.S.R.; Bakier, A. Thermal analysis of natural convection and radiation in porous fins. *Int. Commun. Heat Mass Transf.* **2011**, *38*, 638–645. [\[CrossRef\]](#)
2. Hoseinzadeh, S.; Moafi, A.; Shirkhani, A.; Chamkha, A.J. Numerical Validation Heat Transfer of Rectangular Cross-Section Porous Fins. *J. Thermophys. Heat Transf.* **2019**, *33*, 698–704. [\[CrossRef\]](#)
3. Venkitesh, V.; Mallick, A. Thermal analysis of a convective–conductive–radiative annular porous fin with variable thermal parameters and internal heat generation. *J. Therm. Anal. Calorim.* **2022**, *147*, 1519–1533. [\[CrossRef\]](#)
4. Madhura, K.R.; Babitha; Kalpana, G.; Makinde, O.D. Thermal performance of straight porous fin with variable thermal conductivity under magnetic field and radiation effects. *Heat Transf.* **2020**, *49*, 5002–5019. [\[CrossRef\]](#)
5. Ndlovu, P.L.; Moitsheki, R.J. Steady state heat transfer analysis in a rectangular moving porous fin. *Propuls. Power Res.* **2020**, *9*, 188–196. [\[CrossRef\]](#)
6. Wang, F.; Kumar, R.V.; Sowmya, G.; El-Zahar, E.R.; Prasannakumara, B.; Khan, M.I.; Khan, S.U.; Malik, M.; Xia, W.-F. LSM and DTM-Pade approximation for the combined impacts of convective and radiative heat transfer on an inclined porous longitudinal fin. *Case Stud. Therm. Eng.* **2022**, *35*, 101846. [\[CrossRef\]](#)
7. Aziz, A.; Khani, F. Convection–radiation from a continuously moving fin of variable thermal conductivity. *J. Frankl. Inst.* **2011**, *348*, 640–651. [\[CrossRef\]](#)
8. Sun, Y.; Ma, J. Application of Collocation Spectral Method to Solve a Convective-Radiative Longitudinal Fin with Temperature Dependent Internal Heat Generation, Thermal Conductivity and Heat Transfer Coefficient. *J. Comput. Theor. Nanosci.* **2015**, *12*, 2851–2860. [\[CrossRef\]](#)
9. Dogonchi, A.; Ganji, D. Convection–radiation heat transfer study of moving fin with temperature-dependent thermal conductivity, heat transfer coefficient and heat generation. *Appl. Therm. Eng.* **2016**, *103*, 705–712. [\[CrossRef\]](#)
10. Khan, N.A.; Sulaiman, M.; Kumam, P.; Abu Bakar, M. Thermal Analysis of Conductive-Convection-Radiative Heat Exchangers With Temperature Dependent Thermal Conductivity. *IEEE Access* **2021**, *9*, 138876–138902. [\[CrossRef\]](#)
11. Sarwe, D.U.; Kulkarni, V.S. Thermal behaviour of annular hyperbolic fin with temperature dependent thermal conductivity by differential transformation method and Pade approximant. *Phys. Scr.* **2021**, *96*, 105213. [\[CrossRef\]](#)
12. Roy, P.K.; Mallick, A. Thermal analysis of straight rectangular fin using homotopy perturbation method. *Alex. Eng. J.* **2016**, *55*, 2269–2277. [\[CrossRef\]](#)
13. Ndlovu, P.L. The Significance of Fin Profile and Convective-Radiative Fin Tip on Temperature Distribution in a Longitudinal Fin. *Nano Hybrids Compos.* **2019**, *26*, 93–105. [\[CrossRef\]](#)
14. Gouran, S.; Ghasemi, S.; Mohsenian, S. Effect of internal heat source and non-independent thermal properties on a convective–radiative longitudinal fin. *Alex. Eng. J.* **2022**, *61*, 8545–8554. [\[CrossRef\]](#)
15. Khan, N.A.; Sulaiman, M.; Alshammari, F.S. Heat transfer analysis of an inclined longitudinal porous fin of trapezoidal, rectangular and dovetail profiles using cascade neural networks. *Struct. Multidiscip. Optim.* **2022**, *65*, 251. [\[CrossRef\]](#)
16. Din, Z.U.; Ali, A.; Ullah, S.; Zaman, G.; Shah, K.; Mlaiki, N. Investigation of Heat Transfer from Convective and Radiative Stretching/Shrinking Rectangular Fins. *Math. Probl. Eng.* **2022**, *2022*, e1026698. [\[CrossRef\]](#)
17. Sarwe, D.U.; Kulkarni, V.S. Differential transformation method to determine heat transfer in annular fins. *Heat Transf.* **2021**, *50*, 7949–7971. [\[CrossRef\]](#)
18. Kumar, R.S.V.; Sowmya, G. A novel analysis for heat transfer enhancement in a trapezoidal fin wetted by $\text{MoS}_2 + \text{Fe}_3\text{O}_4 + \text{NiZnFe}_2\text{O}_4$ - methanol based ternary hybrid nanofluid. *Waves Random Complex Media* **2022**, 1–19. [\[CrossRef\]](#)
19. Abdulrahman, A.; Gamaoun, F.; Kumar, R.V.; Khan, U.; Gill, H.S.; Nagaraja, K.; Eldin, S.M.; Galal, A.M. Study of thermal variation in a longitudinal exponential porous fin wetted with $\text{TiO}_2\text{–SiO}_2$ / hexanol hybrid nanofluid using hybrid residual power series method. *Case Stud. Therm. Eng.* **2023**, *43*, 102777. [\[CrossRef\]](#)
20. Jagadeesha, K.C.; Kumar, R.S.V.; Sowmya, G.; Prasannakumara, B.C.; Khan, M.I.; Guedri, K.; Jameel, M.; Galal, A.M. Physical significance of rectangular and hyperbolic annular fin with radiation, convection and nonlinear variable properties. *Int. J. Mod. Phys. B* **2023**, *37*, 2350029. [\[CrossRef\]](#)
21. Altun, A.H.; Ziyilan, O. Experimental investigation of the effects of horizontally oriented vertical sinusoidal wavy fins on heat transfer performance in case of natural convection. *Int. J. Heat Mass Transf.* **2019**, *139*, 425–431. [\[CrossRef\]](#)
22. Luo, C.; Wu, S.; Song, K.; Hua, L.; Wang, L. Thermo-hydraulic performance optimization of wavy fin heat exchanger by combining delta winglet vortex generators. *Appl. Therm. Eng.* **2019**, *163*, 114343. [\[CrossRef\]](#)
23. Song, K.; Hu, D.; Zhang, Q.; Zhang, K.; Wu, X.; Wang, L. Thermal-hydraulic characteristic of a novel wavy fin-and-circle tube heat exchanger with concave curved vortex generators. *Int. J. Heat Mass Transf.* **2022**, *194*, 123023. [\[CrossRef\]](#)
24. Pichi, F.; Ballarin, F.; Rozza, G.; Hesthaven, J.S. An artificial neural network approach to bifurcating phenomena in computational fluid dynamics. *Comput. Fluids* **2023**, *254*, 105813. [\[CrossRef\]](#)
25. Alsaiani, A.O.; Moustafa, E.B.; Alhumade, H.; Abulkhair, H.; Elsheikh, A. A coupled artificial neural network with artificial rabbits optimizer for predicting water productivity of different designs of solar stills. *Adv. Eng. Softw.* **2023**, *175*, 103315. [\[CrossRef\]](#)
26. Kamsuwan, C.; Wang, X.; Seng, L.P.; Xian, C.K.; Piemjaiswang, R.; Piumsombon, P.; Pratumwal, Y.; Otarawanna, S.; Chalermssin-suwan, B. Simulation of nanofluid micro-channel heat exchanger using computational fluid dynamics integrated with artificial neural network. *Energy Rep.* **2023**, *9*, 239–247. [\[CrossRef\]](#)

27. El Jery, A.; Khudhair, A.K.; Abbas, S.Q.; Abed, A.M.; Khedher, K.M. Numerical simulation and artificial neural network prediction of hydrodynamic and heat transfer in a geothermal heat exchanger to obtain the optimal diameter of tubes with the lowest entropy using water and Al_2O_3 /water nanofluid. *Geothermics* **2023**, *107*, 102605. [[CrossRef](#)]
28. Mehmandousti, M.M.; Kowsary, F. Artificial neural network-based multi-objective optimization of cooling of lithium-ion batteries used in electric vehicles utilizing pulsating coolant flow. *Appl. Therm. Eng.* **2023**, *219*, 119385. [[CrossRef](#)]
29. Kuvannarat, T.; Wang, C.-C.; Wongwises, S. Effect of fin thickness on the air-side performance of wavy fin-and-tube heat exchangers under dehumidifying conditions. *Int. J. Heat Mass Transf.* **2006**, *49*, 2587–2596. [[CrossRef](#)]
30. Tian, L.; He, Y.; Tao, Y.; Tao, W. A comparative study on the air-side performance of wavy fin-and-tube heat exchanger with punched delta winglets in staggered and in-line arrangements. *Int. J. Therm. Sci.* **2009**, *48*, 1765–1776. [[CrossRef](#)]
31. Ma, X.; Ding, G.; Zhang, Y.; Wang, K. Airside characteristics of heat, mass transfer and pressure drop for heat exchangers of tube-in hydrophilic coating wavy fin under dehumidifying conditions. *Int. J. Heat Mass Transf.* **2009**, *52*, 4358–4370. [[CrossRef](#)]
32. Lotfi, B.; Sundén, B.; Wang, Q. An investigation of the thermo-hydraulic performance of the smooth wavy fin-and-elliptical tube heat exchangers utilizing new type vortex generators. *Appl. Energy* **2016**, *162*, 1282–1302. [[CrossRef](#)]
33. Liu, X.; Wang, M.; Liu, H.; Chen, W.; Qian, S. Numerical analysis on heat transfer enhancement of wavy fin-tube heat exchangers for air-conditioning applications. *Appl. Therm. Eng.* **2021**, *199*, 117597. [[CrossRef](#)]
34. Xu, P.; Wen, J.; Wang, S.; Chen, Q.; Li, Y. Numerical simulation on flow and heat transfer performances of serrated and wavy fins in plate-fin heat exchanger for hydrogen liquefaction. *Int. J. Hydrog. Energy* **2023**. [[CrossRef](#)]
35. Sertel, H.; Bilen, K. The Effect of Using Sinusoidal Profile in Fins on Thermal Performance. *Int. J. Heat Technol.* **2019**, *37*, 741–750. [[CrossRef](#)]
36. Khaled, A.A. Thermal performance of six different types of wavy-fins. *Int. J. Numer. Methods Heat Fluid Flow* **2015**, *25*, 892–911. [[CrossRef](#)]
37. Kundu, B. Performance and optimum design analysis of longitudinal and pin fins with simultaneous heat and mass transfer: Unified and comparative investigations. *Appl. Therm. Eng.* **2007**, *27*, 976–987. [[CrossRef](#)]
38. Ma, J.; Sun, Y.; Li, B.; Chen, H. Spectral collocation method for radiative–conductive porous fin with temperature dependent properties. *Energy Convers. Manag.* **2016**, *111*, 279–288. [[CrossRef](#)]
39. Pothina, H.; Nagaraja, K.V. Artificial Neural Network and Math behind It. In *Smart Trends in Computing and Communications*; Zhang, Y.-D., Senjyu, T., So-In, C., Joshi, A., Eds.; Springer Nature: Singapore, 2023; pp. 205–221. [[CrossRef](#)]
40. Nagaraja, K.; Pothina, H.; Devi, S.; Reddy, M.; Panda, T.D. An Overview of the Artificial Neural Network-Based Applications and Impact Assessment in COVID-19. *ECS Trans.* **2022**, *107*, 1475–1486. [[CrossRef](#)]

Disclaimer/Publisher’s Note: The statements, opinions and data contained in all publications are solely those of the individual author(s) and contributor(s) and not of MDPI and/or the editor(s). MDPI and/or the editor(s) disclaim responsibility for any injury to people or property resulting from any ideas, methods, instructions or products referred to in the content.